COMPUTATION OF THE VIBRATION MODES OF A REISSNER-MINDLIN LAMINATED PLATE

RICARDO G. DURÁN, RODOLFO RODRÍGUEZ, AND FRANK SANHUEZA

Abstract. This paper deals with the finite element approximation of the vibration modes of a laminated plate modeled by the Reissner-Mindlin equations; DL3 elements are used for the bending terms and standard piecewise linear continuous elements for the in-plane displacements. An *a priori* estimate of the regularity of the solution, independent of the plate thickness, is proved for the corresponding load problem. This allows using the abstract approximation theory for spectral problems to study the convergence of the proposed finite element method. Thus, optimal order error estimates including a double order for the vibration frequencies are obtained under appropriate assumptions. These estimates are independent of the plate thickness, which leads to the conclusion that the method is locking-free. Numerical tests are reported to assess the performance of the method.

1. Introduction

The laminated plates are widely used in engineering practice, for instance in automobile, space, and civil applications. The main motivation for this interest is related to the improved ratio between performances and weight of this kind of plates with respect to homogeneous ones. Several different models of these plates have been proposed. The simplest one is the *Classical Laminated Plate Theory* (CLPT) [13], which is based on the Kirchhoff hypotheses. However, other models arising from the Reissner-Mindlin assumptions are often preferred; they are called *First-order Shear-Deformation Theory* (FSDT) [3].

Locking is a very well known phenomenon in the numerical computation of plate problems. It consists in that very unsatisfactory results are obtained when the thickness is small with respect to the other dimensions of the structure. From the point of view of the numerical analysis, locking reveals itself in that the *a priori* estimates depend on the thickness of the structure in such a way that they degenerate when this parameter becomes small. Several methods based on reduced integration or mixed formulations have been devised to avoid locking in the load plate problem (see [6], for instance). Some of them have been analyzed for the plate vibration problem, as well. For instance, the DL3 and the MITC elements (which

2000 *Mathematics Subject Classification.* Primary 65N25, 74K10, 65N30.

Key words and phrases. Reissner-Mindlin, laminated plates, spectral problems.

The first author was partially supported by Universidad de Buenos Aires under grant X052. Member of CONICET (Argentina).

The second author was partially supported by FONDAP and BASAL projects CMM, Universidad de Chile (Chile).

The third author was supported by a CONICYT fellowship (Chile).

All authors were partially supported by ANPCyT through grant PICT RAÍCES 2006, No. 1307 (Argentina).

were introduced for load problems in [10] and [5], respectively) have been analyzed for vibration problems in [9] and [8], respectively.

Locking-free methods for load problems of laminated plates with several layers all of the same thickness have been analyzed in [2] in a general context. In the present paper we address the corresponding vibration problem. For simplicity, we present the analysis in the case of only two layers. We use the DL3 elements introduced in [10] for the bending terms and standard triangular finite elements for the in-plane displacements. The analysis is made in the framework of the abstract spectral approximation theory for compact operators as stated, for instance, in [4, Section 7]. The goal is to prove optimal order convergence in L^2 and H^1 norms for the eigenfunctions and a double order for the eigenvalues. Moreover, to ensure that the method is locking-free, it has to be proved that the error estimates do not deteriorate as the plate thickness becomes small.

The present analysis is based on the results for load problems for laminated plates from [2] and for the vibration problem for homogeneous plates from [9]. The main difficulty is the need for additional regularity of the solution of the load problem for a Reissner-Mindlin laminated plate. This is the reason why we had to prove new *a priori* estimates for this problem, with constants independent of the plate thickness. This result is interesting by itself, since the error of any numerical method for laminated plates will rely on such an estimate. To the best of the authors knowledge, the obtained estimate had not been proved before. Moreover, the proof of the analogous estimate known for classical Reissner-Mindlin plates (see [1]) does not extend directly to this case. In fact, to extend it, we had to resort to more recent regularity results for formally positive elliptic systems from [12].

The outline of the paper is as follows. In Section 2, we present the mathematical setting of the vibration problem for a laminated plate. The resulting spectral problem is shown to be well posed. The eigenvalues and eigenfunctions are shown to converge to the corresponding ones of the limit problem as the thickness of the laminated plate goes to zero, which corresponds to a Kirchhoff laminated plate. The finite element discretization is introduced in Section 3 and optimal orders of convergence are proved. These estimates are proved to be independent of the plate thickness and this allows us to conclude that the method is locking-free. In Section 4, we report several numerical tests confirming the theoretical results and showing the good performance of the method. The experiments include some cases not covered by the theoretical analysis, where optimal orders of convergence are also attained. Finally, we prove in an Appendix a thickness-independent *a priori* estimate for the regularity of the solution of the corresponding load problem.

Throughout the paper, we will use standard notation for Sobolev and Lebesgue spaces. Moreover, $\|\cdot\|_0$ will denote the standard norm of $L^2(\Omega)$ (or $L^2(\Omega)^n$, as corresponds). Analogously, $\|\cdot\|_k$ will denote the norm of $H^k(\Omega)$ (or $H^k(\Omega)^n$). Finally, C will denote a generic constant, not necessarily the same at each occurrence, but always independent of the plate thickness t, the particular functions involved, and, in Section 3, also independent of the mesh-size.

2. Reissner-Mindlin laminated plate equations

Consider an elastic plate of thickness t with reference configuration $\Omega\times\left(-\frac{t}{2},\frac{t}{2}\right)$, where $\Omega\subset\mathbb{R}^2$ is a convex polygonal domain. The plate is made of two different materials, one occupying the subdomain $\Omega\times\left(-\frac{t}{2},0\right)$ and the other one $\Omega\times\left(0,\frac{t}{2}\right)$.

According to the Reissner-Mindlin model, the plate deformation is described by means of the in-plane and transverse displacements, $u^* = (u_1^*, u_2^*)$ and w^*, respectively, and the rotations $\beta^* = (\beta_1^*, \beta_2^*)$ of its mid-surface Ω. For the forthcoming analysis, we assume that the plate is clamped on its whole boundary $\partial\Omega$.

The vibration problem for such a plate can be formally obtained from the three-dimensional linear elasticity equations as follows: According to the Reissner-Mindlin hypotheses, the admissible displacements at each point are given by

$$(u^*(x) - x_3\beta^*(x), w^*(x)), \qquad x := (x_1, x_2) \in \Omega, \quad x_3 \in \left(-\tfrac{t}{2}, \tfrac{t}{2}\right).$$

Test and trial displacements of this form are taken in the variational formulation of the linear elasticity equations for the vibration problem of the three-dimensional plate. By integrating over the thickness and multiplying the shear term by a correcting factor, one arrives at the following problem (see [16]):

Find $\omega > 0$ and non trivial $(u^*, \beta^*, w^*) \in V$ satisfying

$$\begin{aligned}
&t\left(\mathcal{A}\varepsilon(u^*), \varepsilon(v)\right) + t^2\left[\left(\mathcal{B}\varepsilon(u^*), \varepsilon(\eta)\right) + \left(\mathcal{B}\varepsilon(\beta^*), \varepsilon(v)\right)\right] \\
&+ t^3\left(\mathcal{D}\varepsilon(\beta^*), \varepsilon(\eta)\right) + t\kappa\left(\beta^* - \nabla w^*, \eta - \nabla z\right) \\
&\quad = \omega^2\left\{\frac{t}{2}\left(\rho_1 + \rho_2\right)\left(u^*, v\right) + \frac{t^3}{24}\left(\rho_1 + \rho_2\right)\left(\beta^*, \eta\right)\right. \\
&\qquad \left. + \frac{t}{2}\left(\rho_1 + \rho_2\right)\left(w^*, z\right) + \frac{t^2}{8}\left(\rho_1 - \rho_2\right)\left[\left(\beta^*, v\right) + \left(u^*, \eta\right)\right]\right\} \quad \forall (v, \eta, z) \in V,
\end{aligned}$$

where

$$V := H_0^1(\Omega)^2 \times H_0^1(\Omega)^2 \times H_0^1(\Omega).$$

In the equation above ω is the angular vibration frequency, $(\cdot, \cdot)$ denotes the standard $L^2(\Omega)$ inner product of scalar, vector or tensor fields, as corresponds, and ε is the linear strain tensor defined by $\varepsilon_{ij}(v) := \frac{1}{2}\left(\partial v_i/\partial x_j + \partial v_j/\partial x_i\right)$, $i, j = 1, 2$. Moreover, $\mathcal{A}$, $\mathcal{B}$, and $\mathcal{D}$ are fourth order tensors defined by

$$\mathcal{A}(\tau) := \frac{1}{2}\left(\mathcal{C}_1 + \mathcal{C}_2\right)\tau, \quad \mathcal{B}(\tau) := \frac{1}{8}\left(\mathcal{C}_1 - \mathcal{C}_2\right)\tau, \quad \text{and} \quad \mathcal{D}(\tau) := \frac{1}{24}\left(\mathcal{C}_1 + \mathcal{C}_2\right)\tau,$$

where $\mathcal{C}_1$ and $\mathcal{C}_2$ are the linear elasticity operators on each medium,

$$\mathcal{C}_i\tau := \lambda_i \operatorname{tr}(\tau) I + 2\mu_i\tau, \qquad i = 1, 2,$$

with plane stress Lamé coefficients $\lambda_i := E_i\nu_i/\left(1 - \nu_i^2\right)$ and $\mu_i := E_i/\left[2\left(1 + \nu_i\right)\right]$, E_i being the Young modulus and ν_i the Poisson ratio of each material. Finally $\kappa := k(\mu_1 + \mu_2)/2$ is the shear modulus of the laminated plate, with k a correction factor usually taken as $5/6$, and ρ_i is the density of each material.

We rescale the problem using new variables

$$u := u^*/t, \quad \beta := \beta^*, \quad w =: w^*, \quad \text{and} \quad \lambda_t := \frac{\rho_1 + \rho_2}{2}\frac{\omega^2}{t^2}.$$

The reason for this is that the rescaled variables attain finite non-zero limits as t goes to zero, as will be shown below (cf. Lemma 2.2). We also introduce the scaled shear stress

$$\gamma := \frac{\kappa}{t^2}\left(\beta - \nabla w\right)$$

and the bilinear forms

$$a((u, \beta), (v, \eta)) := \left(\mathcal{A}\varepsilon(u), \varepsilon(v)\right) + \left(\mathcal{B}\varepsilon(u), \varepsilon(\eta)\right) + \left(\mathcal{B}\varepsilon(v), \varepsilon(\beta)\right) + \left(\mathcal{D}\varepsilon(\beta), \varepsilon(\eta)\right)$$

and

$$b_t((u,\beta,w),(v,\eta,z)) := (w,z) + t^2\,(u,v) + \frac{t^2}{12}\,(\beta,\eta) + \frac{\rho_1-\rho_2}{4\,(\rho_1+\rho_2)}t^2\,[(\beta,v)+(u,\eta)]\,.$$

Thus, the plate vibration problem can be rewritten as follows:

Find $\lambda_t > 0$ and non trivial $(u,\beta,w) \in V$ such that

$$\left\{\begin{array}{l} a((u,\beta),(v,\eta)) + (\gamma,\eta-\nabla z) = \lambda_t b_t((u,\beta,w),(v,\eta,z)) \quad \forall (v,\eta,z)\in V,\\ \gamma = \dfrac{\kappa}{t^2}\,(\beta-\nabla w)\,. \end{array}\right. \tag{2.1}$$

All the eigenvalues λ_t of this problem are strictly positive, because of the symmetry of both bilinear forms, the ellipticity of a, which has been proved in [2, Proposition 2.1], and the positiveness of b_t, which can be proved by straightforward computations.

To analyze the approximation of this eigenvalue problem, we introduce the operator

$$T_t : H \longrightarrow H,$$

where

$$H := L^2(\Omega)^2 \times L^2(\Omega)^2 \times L^2(\Omega),$$

defined for $(f,m,g) \in H$ by $T_t(f,m,g) := (u,\beta,w)$, with $(u,\beta,w) \in V$ being the solution to

$$\left\{\begin{array}{l} a((u,\beta),(v,\eta)) + (\gamma,\eta-\nabla z) = b_t((f,m,g),(v,\eta,z)) \quad \forall (v,\eta,z)\in V,\\ \gamma = \dfrac{\kappa}{t^2}\,(\beta-\nabla w)\,. \end{array}\right. \tag{2.2}$$

This is the load problem for the Reissner-Mindlin laminated clamped plate. It is a well posed problem; in fact, the existence and uniqueness of the solution for all $t > 0$ follows from [2, Proposition 2.1].

Because of the symmetry of the bilinear forms a and b_t, the operator T_t is self-adjoint in H endowed with the inner-product $b_t(\cdot,\cdot)$. The norm induced by this inner product is equivalent to the weighted L^2 norm

$$|(v,\eta,z)|_t^2 := t^2\,\|v\|_0^2 + t^2\,\|\eta\|_0^2 + \|z\|_0^2\,, \qquad (v,\eta,z)\in H,$$

with equivalence constants independent of t. On the other hand, because of the compact embedding $H_0^1(\Omega) \hookrightarrow L^2(\Omega)$, T_t is a compact operator. Then, apart from 0, its spectrum consists of a sequence of finite multiplicity real eigenvalues converging to zero. Note that λ_t is an eigenvalue of Problem (2.1) if and only if $\mu_t := 1/\lambda_t$ is an eigenvalue of T_t, with the same multiplicity and corresponding eigenfunctions.

The solution of the load problem (2.2) satisfies the following additional regularity result, which is systematically used in the proofs that follow: $u,\beta \in H^2(\Omega)^2$, $w \in H^2(\Omega)$, $\gamma \in H^1(\Omega)^2$, and there exists a constant $C > 0$, independent of t and (f,m,g), such that

$$\|u\|_2 + \|\beta\|_2 + \|w\|_2 + \|\gamma\|_0 + t\,\|\gamma\|_1 \le C\left(t^2\,\|f\|_0 + t^2\,\|m\|_0 + \|g\|_0\right). \tag{2.3}$$

The proof of this *a priori* estimate is far from being straightforward. In fact, although it is proved by extending similar arguments used for classical homogeneous plates in [1, Theorem 7.1], it needs of some preliminary results. Thus, for the sake of clarity, we postpone this analysis to the Appendix. In particular, the estimate (2.3) is a consequence of Theorem 6.5 from this Appendix (cf. Corollary 6.6).

On the other hand, as a consequence of [7, Theorem 1], it can be shown as in [2, Proposition 2.2] that, when $t \to 0$, the solution (u, β, w) to (2.2) converges to $(u_0, \nabla w_0, w_0)$, where $(u_0, w_0) \in H_0^1(\Omega)^2 \times H_0^2(\Omega)$ satisfies

$$a((u_0, \nabla w_0), (v, \nabla z)) = (g, z) \qquad \forall (v, z) \in H_0^1(\Omega)^2 \times H_0^2(\Omega).$$

This limit problem is well posed and corresponds to the bending of a clamped Kirchhoff-type laminated plate subjected to a (rescaled) transverse load g. The arguments from [6, Section VII.3.1] can be easily adapted to prove that the limit problem above is equivalent to finding $(u_0, \beta_0, w_0) \in V$ such that there exists $\gamma_0 \in H_0(\mathrm{rot}, \Omega)'$ satisfying

$$\left\{ \begin{array}{l} a((u_0, \beta_0), (v, \eta)) + \langle \gamma_0, \eta - \nabla z \rangle = b_0\left((f, m, g), (v, \eta, z)\right) \equiv (g, z) \\ \qquad\qquad\qquad\qquad\qquad\qquad\qquad\qquad\qquad\qquad \forall (v, \eta, z) \in V, \\ \beta_0 - \nabla w_0 = 0, \end{array} \right. \tag{2.4}$$

where $\langle \cdot, \cdot \rangle$ stands for the duality pairing in

$$H_0(\mathrm{rot}, \Omega) := \left\{ \psi \in L^2(\Omega)^2 : \ \mathrm{rot}\, \psi \in L^2(\Omega) \text{ and } \psi \cdot \tau = 0 \text{ on } \partial\Omega \right\},$$

with $\mathrm{rot}\, \psi := \partial_1 \psi_2 - \partial_2 \psi_1$ and τ being a unit vector tangent to $\partial\Omega$. Moreover, the arguments from [6] can also be adapted to prove that this is a well posed mixed problem. Thus, we are allowed to introduce the operator

$$T_0 : H \longrightarrow H,$$

defined for $(f, m, g) \in H$ by $T_0(f, m, g) := (u_0, \beta_0, w_0)$, with (u_0, β_0, w_0) being the solution to problem (2.4).

An *a priori* estimate similar to (2.3) holds for the limit problem (2.4), as well; namely, $u_0, \beta_0 \in H^2(\Omega)^2$, $w_0 \in H^2(\Omega)$, $\gamma_0 \in L^2(\Omega)^2$, and

$$\|u_0\|_2 + \|\beta_0\|_2 + \|w_0\|_2 + \|\gamma_0\|_0 \leq C \|g\|_0 . \tag{2.5}$$

The proof of this estimate is a consequence of Lemma 6.2 from the Appendix (cf. Corollary 6.3).

Now, we may proceed as in [9] to prove an estimate for the convergence of the solution to (2.2) to that to (2.4) as t goes to zero. In fact we have the following result.

Lemma 2.1. *There exists a constant $C > 0$, independent of t, such that*

$$\|(T_t - T_0)(f, m, g)\|_1 \leq Ct\, |(f, m, g)|_t \qquad \forall (f, m, g) \in H.$$

Proof. Repeating the arguments of the proof of Lemma 6.4 from the Appendix we arrive at

$$\|u - u_0\|_1 + \|\beta - \beta_0\|_1 \leq Ct\, \|(f, m, g)\|_0$$

(cf. (6.19)). Next, subtracting the second equation in (2.4) from that in (2.2), we have

$$\gamma = \frac{\kappa}{t^2} \left(\beta - \beta_0 - \nabla(w - w_0)\right).$$

Hence, the estimate above and (2.3) yield

$$\|w - w_0\|_1 \leq \frac{t^2}{\kappa} \|\gamma\|_0 + \|\beta - \beta_0\|_0 \leq Ct\, |(f, m, g)|_{b_t} .$$

Thus, we conclude the proof. □

As a consequence of this lemma, the operator $T_t|_V$ converges in norm to $T_0|_V$. Then, standard properties of separation of isolated parts of the spectrum (see for instance [11]) yield the following result.

Lemma 2.2. *Let $\mu_0 > 0$ be an eigenvalue of T_0 of multiplicity m. Let D be any disc in the complex plane centered at μ_0 and containing no other element of the spectrum of T_0. Then, for t small enough, D contains exactly m eigenvalues of T_t (repeated according to their respective multiplicities). Consequently, each eigenvalue $\mu_0 > 0$ of T_0 is a limit of eigenvalues μ_t of T_t, as t goes to zero.*

3. Finite-element discretization

We restrict our analysis to the DL3 elements introduced in [10], although other finite elements can be analyzed in this same framework. We consider a regular family of triangulations $\{\mathcal{T}_h\}$; as usual, h denotes the mesh-size.

To discretize the rotations, we use standard piecewise linear functions augmented in such a way that they have quadratic tangential components on the boundary of each element. More precisely, for each $T \in \mathcal{T}_h$, let α_i^T, $i = 1, 2, 3$, be its barycentric coordinates and τ_i^T a unit vector tangent to the edge $\alpha_i^T = 0$. Consider the edge-bubble vector fields $\varphi_i^T := \alpha_j^T \alpha_k^T \tau_i^T$, $i, j, k = 1, 2, 3$, all different. The finite element space for the rotations is defined by

$$X_h := \left\{ \eta_h \in H_0^1(\Omega)^2 : \ \eta_h|_T \in \mathcal{P}_1^2 \oplus \langle \varphi_1^T, \varphi_2^T, \varphi_3^T \rangle \quad \forall T \in \mathcal{T}_h \right\}.$$

We use standard piecewise linear elements for the displacements; namely,

$$W_h := \{ z_h \in H_0^1(\Omega) : \ z_h|_T \in \mathcal{P}_1, \ \forall T \in \mathcal{T}_h \}$$

for the transverse displacements and

$$U_h := W_h^2$$

for the in-plane displacements. Thus, the finite element discretization of the space V is defined by

$$V_h := U_h \times X_h \times W_h.$$

For the numerical method, we also need the so called *reduction operator*

$$R : H^1(\Omega)^2 \cap H_0(\mathrm{rot}, \Omega) \longrightarrow \Gamma_h,$$

where Γ_h is the lowest-order rotated Raviart-Thomas space (see [14])

$$\Gamma_h := \left\{ \psi_h \in H_0(\mathrm{rot}, \Omega) : \ \psi_h|_T \in \mathcal{P}_0^2 \oplus (-x_2, x_1)\mathcal{P}_0 \quad \forall T \in \mathcal{T}_h \right\}.$$

This reduction operator is uniquely determined by

$$\int_\ell R\psi \cdot \tau_\ell = \int_\ell \psi \cdot \tau_\ell, \qquad \psi \in H^1(\Omega)^2 \cap H_0(\mathrm{rot}, \Omega),$$

for every edge ℓ of the triangulation (τ_ℓ being a unit tangent vector along ℓ).

Now we are in a position to write the finite element approximation of the plate vibration problem (2.1):

Find $\lambda_{th} > 0$ and non trivial $(u_h, \beta_h, w_h) \in V_h$ such that

$$\left\{ \begin{array}{l} a((u_h, \beta_h), (v_h, \eta_h)) + (\gamma_h, R\eta_h - \nabla v_h) \\ \qquad\qquad = \lambda_{th} b_t((u_h, \beta_h, w_h), (v_h, \eta_h, z_h)) \quad \forall (v_h, \eta_h, z_h) \in V_h, \\ \gamma_h = \dfrac{\kappa}{t^2} \left(R\beta_h - \nabla w_h \right). \end{array} \right. \tag{3.1}$$

Notice that the method is non conforming since consistency terms arise because of the reduction operator.

As in the continuous case, we introduce the operator

$$T_{th} : H \longrightarrow H,$$

defined for $(f, m, g) \in H$ by $T_{th}(f, m, g) := (u_h, \beta_h, w_h)$, with $(u_h, \beta_h, w_h) \in V_h$ being the solution to the corresponding finite element discretization of the load problem (2.2), namely,

$$\begin{cases} a((u_h, \beta_h), (v_h, \eta_h)) + (\gamma_h, R\eta_h - \nabla z_h) = b_t((f, m, g), (v_h, \eta_h, z_h)) \\ \qquad\qquad\qquad\qquad\qquad\qquad\qquad\qquad \forall (v_h, \eta_h, z_h) \in V_h, \\ \gamma_h = \dfrac{\kappa}{t^2}\,(R\beta_h - \nabla w_h). \end{cases}$$

The existence and uniqueness of the solution to this problem follows easily from the ellipticity of a. Once more λ_{th} is an eigenvalue of problem (3.1) if and only if $\mu_{th} := 1/\lambda_{th}$ is a strictly positive eigenvalue of T_{th} with the same multiplicity and corresponding eigenfunctions.

For $t > 0$ fixed, the spectral approximation theory for compact operators (cf. [4]) can be readily applied to prove convergence of the eigenpairs of T_{th} to those of T_t. However, further considerations are needed to show that the error estimates do not deteriorate as t becomes small. With this goal, we will make use of the following result, which will lead to optimal error estimates in the H^1 norm for displacements and rotations.

Lemma 3.1. *There exists a constant C, independent of t and h, such that*

$$\|(T_t - T_{th})\,(f, m, g)\|_1 \le Ch\,|(f, m, g)|_t \qquad \forall (f, m, g) \in H.$$

Proof. Let $(f, m, g) \in H$, $(u, \beta, w) := T_t(f, m, g)$, and $(u_h, \beta_h, w_h) := T_{th}(f, m, g)$. The arguments given in the proof of [2, Proposition 3.2] for pure transverse loads (i.e., $f = 0$ and $m = 0$) extend easily to our case yielding

$$\begin{aligned} \|u - u_h\|_1 + \|\beta - \beta_h\|_1 + \|w - w_h\|_1 + t\,\|\gamma - \gamma_h\|_0 \\ \le Ch\,(\|u\|_2 + \|\beta\|_2 + \|\gamma\|_0 + t\,\|\gamma\|_1)\,. \end{aligned}$$

Thus, the lemma follows from this inequality and (2.3). □

As a consequence of this lemma, $T_{th}|_V$ converges in norm to $T_t|_V$. In fact, for any fixed $t \in (0, t_{\max})$, we have $|\cdot|_t \le t_{\max}\,\|\cdot\|_1$ and hence the lemma yields

$$\|(T_t - T_{th})\,(f, m, g)\|_1 \le Ch\,\|(f, m, g)\|_1 \qquad \forall (f, m, g) \in V. \tag{3.2}$$

Consequently, if μ_t is an eigenvalue of T_t with multiplicity m, then exactly m eigenvalues of T_{th} (repeated according to their respective multiplicities) converge to μ_t as h goes to zero (see [11]). The following theorem shows that, under mild assumptions, optimal t-independent error estimates in the H^1 norm are valid for the eigenfunctions.

Theorem 3.2. *Let μ_t be an eigenvalue of T_t converging to a simple eigenvalue μ_0 of T_0, as t goes to zero. Let μ_{th} be the eigenvalue of T_{th} that converges to μ_t as h goes to zero. Let (u, β, w) and (u_h, β_h, w_h) be the corresponding eigenfunctions conveniently normalized. Then, for t and h small enough,*

$$\|(u, \beta, w) - (u_h, \beta_h, w_h)\|_1 \le Ch,$$

with a constant C independent of t and h.

Proof. The inequality of the theorem is a direct consequence of the estimate (3.2) and [4, Theorem 7.1], with a constant C depending on the constant in (3.2) (which is independent of t) and on the inverse of the distance of μ_t to the rest of the spectrum of T_t. Now, according to Lemma 2.2, for t small enough, this distance can be bounded below in terms of the distance of μ_0 to the rest of the spectrum of T_0, which obviously does not depend on t. Thus, we conclude the proof. □

The following lemma is the basic tool to prove a double order of convergence for the eigenvalues.

Lemma 3.3. *There exists a constant C, independent of t and h, such that*

$$\|(T_t - T_{th})(f,m,g)\|_0 \le Ch^2 \,|(f,m,g)|_t \qquad \forall (f,m,g) \in H.$$

Proof. We do not include it, since it is a straightforward modification of the proof of [9, Lemma 3.4]. □

Theorem 3.4. *Let μ_t and μ_{th} be as in Theorem 3.2. Then, for t and h small enough,*

$$|\mu_t - \mu_{th}| \le Ch^2,$$

with a constant C independent of t and h.

Proof. Let (u,β,w) be an eigenfunction corresponding to μ_t normalized in the norm induced by b_t. Applying [4, Theorem 7.3] and taking into account that T and T_h are self-adjoint with respect to b_t, we have

$$|\mu_t - \mu_{th}| \le C\left[b_t((T_t - T_{th})(u,\beta,w),(u,\beta,w)) + |(T_t - T_{th})(u,\beta,w)|_t^2\right], \tag{3.3}$$

with a constant C depending on the inverse of the distance of μ_t to the rest of the spectrum of T_t. By repeating the arguments in the proof of Theorem 3.2 we observe that, for t small enough, this constant can be chosen independent of t. Thus, since $|\cdot|_t \le C\,\|\cdot\|_0$, using the estimate from Lemma 3.3 in (3.3), we conclude the proof. □

Another consequence of Lemma 3.3 is a double order of convergence for the eigenfunctions in the L^2-norm.

Theorem 3.5. *Let μ_t, μ_{th}, (u,β,w) and (u_h,β_h,w_h) be as in Theorem 3.2. Then, for t and h small enough,*

$$\|(u,\beta,w) - (u_h,\beta_h,w_h)\|_0 \le Ch^2,$$

with a constant C independent of t and h.

Proof. Since $|\cdot|_t \le C\,\|\cdot\|_0$, the arguments in the proof of Theorem 3.2 can be repeated using $\|\cdot\|_0$ instead of $\|\cdot\|_1$ and the estimate from Lemma 3.3 instead of (3.2). □

4. Numerical experiments

We report in this section some numerical results obtained with a code which implements the method analyzed above. The aim of this numerical experimentation is two-fold: to confirm the theoretical results and to assess the performance of the method.

4.1. **Test 1: A simply supported rectangular plate with a known analytical solution. Validation.** The aim of this first test is to validate the computer code and to corroborate the error estimates proved in the previous section. With this purpose, we applied the method to a problem with a known analytical solution: a rectangular simple supported plate (see [15, 16]). This test allowed us to calculate the error of the different quantities computed with our code. Moreover, it shows that the method is able to deal with other kind of boundary conditions, although the theoretical analysis has been made just for clamped plates.

If the domain of the simply supported plate is the rectangle $\Omega := (0, a) \times (0, b)$, then the eigenfunctions are given by

$$u = \begin{bmatrix} \hat{u}_1 \cos \frac{k\pi x}{a} \sin \frac{l\pi y}{b} \\ \hat{u}_2 \sin \frac{k\pi x}{a} \cos \frac{l\pi y}{b} \end{bmatrix}, \quad w = \hat{w} \sin \frac{k\pi x}{a} \sin \frac{l\pi y}{b}, \quad \beta = \begin{bmatrix} \hat{\beta}_1 \cos \frac{k\pi x}{a} \sin \frac{l\pi y}{b} \\ \hat{\beta}_2 \sin \frac{k\pi x}{a} \cos \frac{l\pi y}{b} \end{bmatrix}, \tag{4.1}$$

$k, l \in \mathbb{N}$. The constants $\hat{u}_1$, $\hat{u}_2$, $\hat{w}$, $\hat{\beta}_1$, and $\hat{\beta}_2$, as well as the corresponding eigenvalues, can be obtained as follows: For each pair $(k, l) \in \mathbb{N}^2$, the terms (4.1) must be plugged into (2.1), written in strong form. This leads to a 5×5 generalized eigenvalue problem whose eigenvectors are $(\hat{u}_1, \hat{u}_2, \hat{w}, \hat{\beta}_1, \hat{\beta}_2)^{\mathrm{t}}$ and whose eigenvalues are the ones we are looking for.

We applied the method to a plate of length $a = 6\,\mathrm{m}$, width $b = 4\,\mathrm{m}$, and thickness $t = 0.1\,\mathrm{m}$. We used the following physical parameters:

$$\begin{aligned} &E_1 = 1.440 \times 10^{11}\,\mathrm{N/m^2}, && \nu_1 = 0.35, && \rho_1 = 7700\,\mathrm{kg/m^3}, \\ &E_2 = 0.144 \times 10^{11}\,\mathrm{N/m^2}, && \nu_2 = 0.30, && \rho_2 = 770\,\mathrm{kg/m^3}. \end{aligned}$$

Finally, we took $\kappa = 5/6$ as correction factor for this and all the other tests.

We used uniform meshes obtained by refining the coarse one shown in Figure 1. The refinement parameter N is the number of layers of elements through the width of the plate.

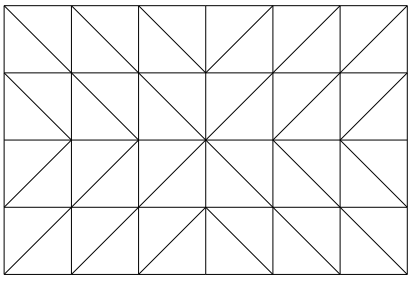

FIGURE 1. Rectangular plate. Finite element coarse mesh ($N = 4$).

Table 1 shows the six lowest vibration frequencies computed with the method on four successively refined meshes. The table also includes the corresponding exact values obtained from the analytical solution and the computed order of convergence for each one.

A quadratic order of convergence can be clearly observed for all the vibration frequencies, which corresponds to an optimal double order according to the degree of the finite elements used.

TABLE 1. Test 1: Lowest vibration frequencies of a simply supported laminated rectangular plate.

Mode	$N = 8$	$N = 16$	$N = 32$	$N = 64$	Exact	Order
ω_1	84.605	83.368	83.066	82.992	82.967	2.02
ω_2	166.169	161.063	159.829	159.527	159.427	2.03
ω_3	272.770	259.194	255.911	255.102	254.834	2.02
ω_4	308.314	291.870	287.894	286.918	286.595	2.02
ω_5	361.027	338.177	332.772	331.458	331.026	2.04
ω_6	514.209	471.247	461.043	458.564	457.749	2.04

Figure 2 shows the error curves in L^2 norm and H^1 seminorm of the in-plane and the transverse displacements, u and w, respectively, for the eigenfunction corresponding to the lowest vibration frequency ω_1.

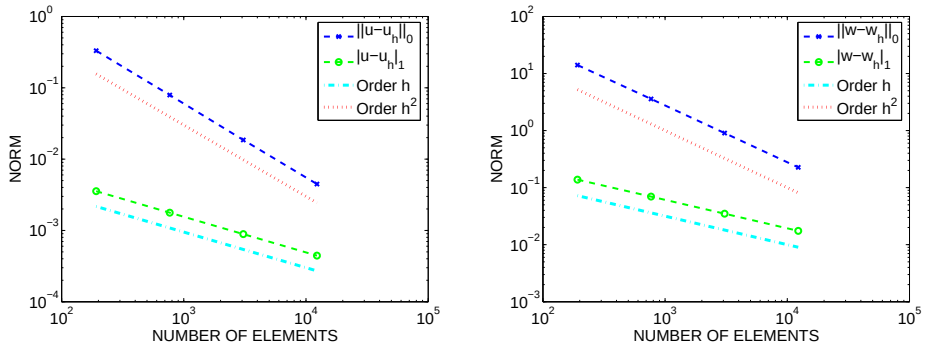

FIGURE 2. Test 1: Error curves for in-plane displacements (left) and transverse displacements (right); log-log plots of the corresponding norms versus the number of elements.

A quadratic order in L^2 and a linear order in H^1 can be clearly observed for both displacements. Once more, this corresponds to the optimal orders according to the degree of the finite elements.

4.2. **Test 2: A clamped rectangular plate. Testing the locking-free character of the method.** The main goal of this test is to confirm experimentally that the method is locking-free, as was proved in the previous section. With this purpose, we chose a problem lying in the theoretical framework: a plate clamped on its whole boundary.

We used a rectangular plate with the same dimensions and physical parameters as in the previous test. We also used the same meshes.

First, we computed the lowest vibration frequencies of the plate on each mesh. Since no analytical solution is available in this case, for each vibration mode, we extrapolated a more accurate approximation of the frequency and estimated the order of convergence by means of a least square fitting.

Table 2 shows the six lowest vibration frequencies computed on different meshes, the estimated order of convergence and the extrapolated more accurate value of each frequency.

TABLE 2. Test 2: Lowest vibration frequencies of a clamped laminated rectangular plate.

Mode	$N = 8$	$N = 16$	$N = 32$	$N = 64$	Order	Extrapolated
ω_1	161.136	157.902	157.095	156.898	2.01	156.831
ω_2	255.847	245.336	242.757	242.128	2.03	241.924
ω_3	418.592	391.593	384.980	383.358	2.03	382.835
ω_4	419.684	393.806	387.352	385.762	2.01	385.237
ω_5	518.006	475.120	464.831	462.331	2.06	461.574
ω_6	667.968	603.579	587.688	583.781	2.02	582.499

Once more, a double order of convergence can be readily observed for all the vibration frequencies.

Next, we tested whether the method remains locking-free as the thickness becomes small. For this test, we took clamped plates with the same physical parameters and dimensions as above, except for the thickness for which we used different values ranging from $t = 0.1\,\mathrm{m}$ to $0.1\,\mathrm{mm}$.

To allow for comparison, we report normalized frequencies $\hat{\omega} := \omega/t$. Table 3 shows the computed lowest vibration frequency of clamped rectangular laminated plates with decreasing values of the thickness. Once more, the table includes the estimated orders of convergence and extrapolated frequencies. We also report on the last row the extrapolated limit values corresponding to $t = 0$ (i.e., the Kirchhoff model).

TABLE 3. Test 2: Normalized lowest frequency $\hat{\omega}_1$ of clamped laminated rectangular plates with varying thickness.

Thickness	$N = 8$	$N = 16$	$N = 24$	$N = 32$	Order	Extrapolated
$t = 0.1\,\mathrm{m}$	1611.365	1579.017	1573.019	1570.948	2.00	1568.239
$t = 0.01\,\mathrm{m}$	1616.810	1584.050	1577.875	1575.707	1.97	1572.859
$t = 0.001\,\mathrm{m}$	1616.866	1584.103	1577.928	1575.759	1.97	1572.883
$t = 0.0001\,\mathrm{m}$	1616.865	1584.103	1577.926	1575.762	1.97	1572.883
$t = 0$ (extr.)	1616.866	1584.103	1577.927	1575.761	1.97	1572.883

We observe that the method is perfectly locking-free, and that the quadratic order of convergence is preserved even for extremely small values of the thickness.

4.3. **Test 3: A clamped circular plate. Robustness of the plate model and the finite element method.** The aim of this test is to assess the efficiency of the Reissner-Mindlin laminated plate model by comparing their results with those obtained from the 3D elasticity equations. In particular, we are interested in exhibiting the robustness of the model, as well as that of the proposed finite element method, when applied to laminates with very different physical parameters. With this purpose, we applied the method to a problem whose corresponding 3D equations can be accurately solved. This is the reason why we chose a circular plate, whose axisymmetric vibration modes can be efficiently computed from the corresponding equations in cylindrical coordinates.

We used a clamped circular plate with diameter $d = 2\,\mathrm{m}$ and thickness $t = 0.1\,\mathrm{m}$. First, we took the same physical parameters as in the other experiments. We used

quasiuniform meshes as that shown in Figure 3. The refinement parameter N is in this case the number of elements on each quarter of the circle.

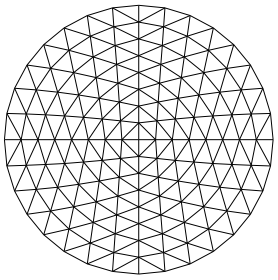

FIGURE 3. Circular plate. Finite element mesh ($N = 8$).

On the other hand, by taking advantage of the cylindrical symmetry, the three-dimensional problem reduces to a two-dimensional one posed on a meridional section of the plate. Thus, we also computed the axisymmetric vibration modes by means of another code based on a standard finite element discretization of the 3D elasticity equations in cylindrical coordinates. Also in this case we used successively refined meshes and obtained a very accurate approximation of the vibrations frequencies by extrapolation.

We report in Table 4 the results for a couple of axisymmetric modes, which, for this plate, correspond to the lowest and the sixth vibration frequencies. The table includes again the extrapolated values of the frequencies and the estimated orders of convergence, as well. It also includes on the last column the values obtained with the axisymmetric 3D code.

TABLE 4. Test 3: Lowest vibration frequencies of axisymmetric modes of a clamped laminated circular plate; Young moduli ratio $E_1/E_2 = 10$.

Mode	$N = 4$	$N = 8$	$N = 16$	$N = 32$	Order	Extrapolated	3D
ω_1	968.270	945.923	940.395	939.020	2.01	938.571	935.748
ω_6	3908.732	3628.509	3559.984	3543.051	2.03	3537.664	3489.815

It can be seen from this table that the disparity between both extrapolated values is very small indeed, which is merely a confirmation of the accuracy of the Reissner-Mindlin laminated plate model.

Next, we tested the robustness of the model applied to laminates with physical parameters of very different scales. With this aim, we computed the vibration modes of a plate identical to the previous one, except for the fact that the Young modulus of the second material is now $E_2 = 0.144 \times 10^8\,\mathrm{N/m^2}$. Therefore, the ratio between the Young moduli of each material is 10^4.

We report in Table 5 the results for this plate analogous to those of the previous table.

Once more, an excellent agreement between both models can be clearly observed, despite the disparity of the Young modulus of each material. Other non reported

TABLE 5. Test 3: Lowest vibration frequencies of axisymmetric modes of a clamped laminated circular plate; Young moduli ratio $E_1/E_2 = 10^4$.

Mode	$N = 4$	$N = 8$	$N = 16$	$N = 32$	Order	Extrapolated	3D
ω_1	671.490	650.794	645.813	644.582	2.05	644.206	645.057
ω_2	2810.616	2540.776	2478.636	2463.491	2.11	2459.352	2425.412

tests demonstrate the robustness of the method for the Reissner-Mindlin laminated plate model with respect to the remaining physical parameters.

Finally, Figures 4 and 5 show the transverse displacement fields computed with the Reissner-Mindlin plate model for the two vibration modes reported in Table 5. The figures also show the corresponding meridional plate sections of each mode computed with the axisymmetric 3D code.

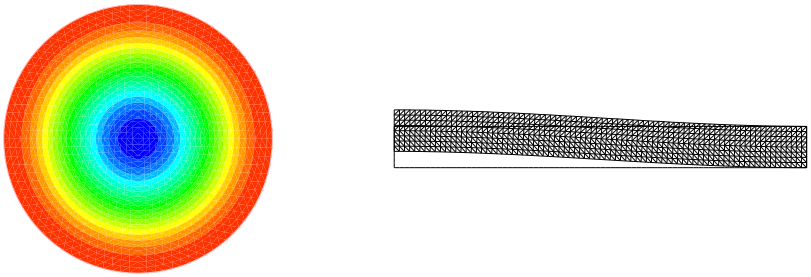

FIGURE 4. Test 3: Lowest axisymmetric vibration mode ω_1 of a clamped laminated circular plate with Young moduli ratio $E_1/E_2 = 10^4$; transverse displacement field (left) and meridional cross section (right).

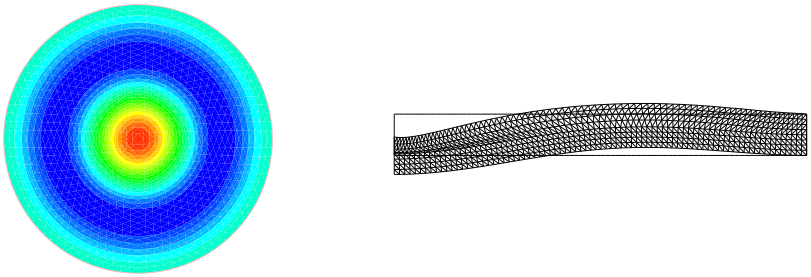

FIGURE 5. Test 3: Second lowest axisymmetric vibration mode ω_6 of a clamped laminated circular plate with Young moduli ratio $E_1/E_2 = 10^4$; transverse displacement field (left) and meridional cross section (right).

5. Conclusions

We analyzed the problem of computing the vibration modes of a clamped laminated plate modeled by Reissner-Mindlin equations. We considered a finite-element method based on DL3 elements for the bending terms and standard triangular piecewise linear elements for the in-plane displacements. We proved optimal order of convergence in H^1 and L^2 for displacements and rotations, as well as a double order for the eigenvalues. We also proved that the error estimates do not deteriorate as the thickness becomes small, which imply that the method is locking-free. The keypoint of the proof is an *a priori* estimate for the regularity of the solution of the corresponding load problem.

We reported numerical experiments confirming the theoretical results. Moreover, these experiments show the robustness with respect to the physical parameters of both, the Reissner-Mindlin laminated plate model and the proposed method. Finally, the experiments also show that the method works for more general boundary conditions.

6. Appendix

In this Appendix we will obtain an *a priori* estimate for the solution of the load problem (2.2) similar to the one valid for classical homogeneous Reissner-Mindlin plates. With this purpose, first we prove the following auxiliary result.

Lemma 6.1. *Let Ω be a convex polygonal domain in the plane. Given $F, G \in L^2(\Omega)^2$, let $(u,\beta) \in H_0^1(\Omega)^2 \times H_0^1(\Omega)^2$ be the unique solution of*

$$a((u,\beta),(v,\eta)) = (F,v) + (G,\eta) \qquad \forall (v,\eta) \in H_0^1(\Omega)^2 \times H_0^1(\Omega)^2. \tag{6.1}$$

Then, $(u,\beta) \in H^2(\Omega)^2 \times H^2(\Omega)^2$ and

$$\|u\|_2 + \|\beta\|_2 \le C\left(\|F\|_0 + \|G\|_0\right),$$

with a constant C independent of F ad G.

Proof. We will resort to additional regularity results from [12, Section 8.6] regarding Dirichlet problems for elliptic systems. In this reference it is proved that the strip of the complex plane $|\mathrm{Re}\,\lambda| \le 1$ is free of eigenvalues of the Mellin symbol, which implies H^2 regularity for L^2 right hand sides, provided the elliptic system (6.1) is *formally positive*.

Let us recall that *formally positiveness* means in our case that if the bilinear form of the elliptic system is written as follows,

$$a((u,\beta),(v,\eta)) = \sum_{i,j=1}^{2} \boldsymbol{A}_{ij}\, \partial_i \boldsymbol{U}\, \partial_j \boldsymbol{V}, \tag{6.2}$$

with

$$\boldsymbol{U} := \begin{bmatrix} u \\ \beta \end{bmatrix} : \Omega \longrightarrow \mathbb{R}^4, \qquad \boldsymbol{V} := \begin{bmatrix} v \\ \eta \end{bmatrix} : \Omega \longrightarrow \mathbb{R}^4,$$

and $\boldsymbol{A}_{ij} \in \mathbb{R}^{4\times 4}$, then

$$\boldsymbol{A} := \begin{bmatrix} \boldsymbol{A}_{11} & \boldsymbol{A}_{12} \\ \boldsymbol{A}_{21} & \boldsymbol{A}_{12} \end{bmatrix} \in \mathbb{R}^{8\times 8}$$

is a symmetric positive definite matrix.

In our case

$$
\begin{aligned}
a((u,\beta),(v,\eta)) = {} & \bar\lambda_1\,(\operatorname{tr}\varepsilon(u),\operatorname{tr}\varepsilon(v)) + 2\bar\mu_1\,(\varepsilon(u),\varepsilon(v)) \\
& + \bar\lambda_2\,(\operatorname{tr}\varepsilon(u),\operatorname{tr}\varepsilon(\eta)) + 2\bar\mu_2\,(\varepsilon(u),\varepsilon(\eta)) \\
& + \bar\lambda_2\,(\operatorname{tr}\varepsilon(v),\operatorname{tr}\varepsilon(\beta)) + 2\bar\mu_2\,(\varepsilon(v),\varepsilon(\beta)) \\
& + \bar\lambda_3\,(\operatorname{tr}\varepsilon(\beta),\operatorname{tr}\varepsilon(\eta)) + 2\bar\mu_3\,(\varepsilon(\beta),\varepsilon(\eta))\,,
\end{aligned} \tag{6.3}
$$

with

$$
\begin{aligned}
&\bar\lambda_1 = \frac{\lambda_1+\lambda_2}{2}, \qquad \bar\lambda_2 = \frac{\lambda_1-\lambda_2}{8}, \qquad \bar\lambda_3 = \frac{\lambda_1+\lambda_2}{24}, \\
&\bar\mu_1 = \frac{\mu_1+\mu_2}{2}, \qquad \bar\mu_2 = \frac{\mu_1-\mu_2}{8}, \qquad \bar\mu_3 = \frac{\mu_1+\mu_2}{24}.
\end{aligned} \tag{6.4}
$$

If (6.3) is directly written in the form (6.2), the resulting matrix $\boldsymbol{A}$ is not positive definite. However, using the fact that

$$
\begin{aligned}
&\int_\Omega \partial_2 u_1\,\partial_1\eta_2 = \int_\Omega \partial_1 u_1\,\partial_2\eta_2, && \int_\Omega \partial_1 u_2\,\partial_2\eta_1 = \int_\Omega \partial_2 u_2\,\partial_1\eta_1, \\
&\int_\Omega \partial_2\beta_1\,\partial_1 v_2 = \int_\Omega \partial_1\beta_1\,\partial_2 v_2, \qquad \text{and} && \int_\Omega \partial_1\beta_2\,\partial_2 v_1 = \int_\Omega \partial_2\beta_2\,\partial_1 v_1
\end{aligned}
$$

(which is proved by a double integration by parts), (6.3) can also be written in the form (6.2) with

$$
\boldsymbol{A}_{11} = \begin{bmatrix} \bar\lambda_1+2\bar\mu_1 & 0 & \bar\lambda_2+2\bar\mu_2 & 0 \\ 0 & \bar\mu_1 & 0 & \bar\mu_2 \\ \bar\lambda_2+2\bar\mu_2 & 0 & \bar\lambda_3+2\bar\mu_3 & 0 \\ 0 & \bar\mu_2 & 0 & \bar\mu_3 \end{bmatrix}, \quad \boldsymbol{A}_{22} = \begin{bmatrix} \bar\mu_1 & 0 & \bar\mu_2 & 0 \\ 0 & \bar\lambda_1+2\bar\mu_1 & 0 & \bar\lambda_2+2\bar\mu_2 \\ \bar\mu_2 & 0 & \bar\mu_3 & 0 \\ 0 & \bar\lambda_2+2\bar\mu_2 & 0 & \bar\lambda_3+2\bar\mu_3 \end{bmatrix},
$$

and

$$
\boldsymbol{A}_{12} = \boldsymbol{A}_{21}^{\mathrm{t}} = \begin{bmatrix} 0 & \bar\lambda_1+\bar\mu_1 & 0 & \bar\lambda_2+\bar\mu_2 \\ 0 & 0 & 0 & 0 \\ 0 & \bar\lambda_2+\bar\mu_2 & 0 & \bar\lambda_3+\bar\mu_3 \\ 0 & 0 & 0 & 0 \end{bmatrix}.
$$

There only remains to prove that $\boldsymbol{A}$ is positive definite. With this purpose, we write $\boldsymbol{A} = \boldsymbol{B}_1 + \boldsymbol{B}_2$ with

$$
\boldsymbol{B}_1 := \begin{bmatrix} 2\bar\mu_1 & 0 & 2\bar\mu_2 & 0 & 0 & \bar\mu_1 & 0 & \bar\mu_2 \\ 0 & \bar\mu_1 & 0 & \bar\mu_2 & 0 & 0 & 0 & 0 \\ 2\bar\mu_2 & 0 & 2\bar\mu_3 & 0 & 0 & \bar\mu_2 & 0 & \bar\mu_3 \\ 0 & \bar\mu_2 & 0 & \bar\mu_3 & 0 & 0 & 0 & 0 \\ 0 & 0 & 0 & 0 & \bar\mu_1 & 0 & \bar\mu_2 & 0 \\ \bar\mu_1 & 0 & \bar\mu_2 & 0 & 0 & 2\bar\mu_1 & 0 & 2\bar\mu_2 \\ 0 & 0 & 0 & 0 & \bar\mu_2 & 0 & \bar\mu_3 & 0 \\ \bar\mu_2 & 0 & \bar\mu_3 & 0 & 0 & 2\bar\mu_2 & 0 & 2\bar\mu_3 \end{bmatrix}
$$

and

$$\boldsymbol{B}_2 := \begin{bmatrix} \bar\lambda_1 & 0 & \bar\lambda_2 & 0 & 0 & \bar\lambda_1 & 0 & \bar\lambda_2 \\ 0 & 0 & 0 & 0 & 0 & 0 & 0 & 0 \\ \bar\lambda_2 & 0 & \bar\lambda_3 & 0 & 0 & \bar\lambda_2 & 0 & \bar\lambda_3 \\ 0 & 0 & 0 & 0 & 0 & 0 & 0 & 0 \\ 0 & 0 & 0 & 0 & 0 & 0 & 0 & 0 \\ \bar\lambda_1 & 0 & \bar\lambda_2 & 0 & 0 & \bar\lambda_1 & 0 & \bar\lambda_2 \\ 0 & 0 & 0 & 0 & 0 & 0 & 0 & 0 \\ \bar\lambda_2 & 0 & \bar\lambda_3 & 0 & 0 & \bar\lambda_2 & 0 & \bar\lambda_3 \end{bmatrix}.$$

We observe that $\boldsymbol{B}_1$ is positive definite. In fact, reordering rows and columns of $\boldsymbol{B}_1$, we obtain the block diagonal matrix

$$\widehat{\boldsymbol{B}}_1 := \begin{bmatrix} \boldsymbol{C}_1 & \boldsymbol{O} \\ \boldsymbol{O} & \boldsymbol{C}_2 \end{bmatrix},$$

with

$$\boldsymbol{C}_1 := \begin{bmatrix} 2\boldsymbol{D}_1 & \boldsymbol{D}_1 \\ \boldsymbol{D}_1 & 2\boldsymbol{D}_1 \end{bmatrix}, \qquad \boldsymbol{C}_2 := \begin{bmatrix} \boldsymbol{D}_1 & \boldsymbol{O} \\ \boldsymbol{O} & \boldsymbol{D}_1 \end{bmatrix}, \qquad \text{and} \qquad \boldsymbol{D}_1 := \begin{bmatrix} \bar\mu_1 & \bar\mu_2 \\ \bar\mu_2 & \bar\mu_3 \end{bmatrix}.$$

Using (6.4), it is simple to show that $\bar\mu_1\bar\mu_3 - \bar\mu_2^2 > 0$. Hence, $\boldsymbol{D}_1$ is positive definite. Therefore, elementary computations show that $\boldsymbol{C}_1$, $\boldsymbol{C}_2$, and consequently $\widehat{\boldsymbol{B}}_1$ and $\boldsymbol{B}_1$, are positive definite, too.

On the other hand, $\boldsymbol{B}_2$ is positive semi-definite. In fact, reordering rows and columns of $\boldsymbol{B}_2$, we obtain

$$\widehat{\boldsymbol{B}}_2 = \begin{bmatrix} \boldsymbol{C}_3 & \boldsymbol{O} \\ \boldsymbol{O} & \boldsymbol{O} \end{bmatrix}, \qquad \text{with} \qquad \boldsymbol{C}_3 := \begin{bmatrix} \boldsymbol{D}_2 & \boldsymbol{D}_2 \\ \boldsymbol{D}_2 & \boldsymbol{D}_2 \end{bmatrix} \qquad \text{and} \qquad \boldsymbol{D}_2 := \begin{bmatrix} \bar\lambda_1 & \bar\lambda_2 \\ \bar\lambda_2 & \bar\lambda_3 \end{bmatrix}.$$

The matrix $\boldsymbol{D}_2$ is positive definite because, using again (6.4), we have $\bar\lambda_1\bar\lambda_3 - \bar\lambda_2^2 > 0$. Therefore, $\boldsymbol{C}_3$ and consequently $\widehat{\boldsymbol{B}}_2$ and $\boldsymbol{B}_2$ are positive semi-definite, too. Thus, $\boldsymbol{A} = \boldsymbol{B}_1 + \boldsymbol{B}_2$ is positive definite and we conclude the proof. □

Now we are in a position to prove that the solutions of the load problems for laminated and classical homogeneous Reissner-Mindlin clamped plates have the same regularity. With this aim, we adapt the arguments from the proof of [1, Theorem 7.1].

For any $t > 0$ and $(f, m, g) \in H$, let $(u, \beta, w) \in V$ and $\gamma \in L^2(\Omega)$ be the solution to

$$\text{(6.5)} \quad \begin{cases} a((u,\beta),(v,\eta)) + (\gamma, \eta - \nabla z) = (f, v) + (m, \eta) + (g, z) \quad \forall (v, \eta, z) \in V, \\ \gamma = \dfrac{\kappa}{t^2}\,(\beta - \nabla w)\,. \end{cases}$$

Consider the Helmholtz decomposition of the shear term $\gamma \in H_0(\mathrm{rot}, \Omega)$:

$$\gamma = \nabla r + \mathrm{curl}\, p. \tag{6.6}$$

with $r \in H_0^1(\Omega)$ and $p \in H^1(\Omega)/\mathbb{R}$. Using this decomposition in (6.5), this problem turns out equivalent to finding $r, w \in H_0^1(\Omega)$, $u, \beta \in H_0^1(\Omega)^2$, and $p \in H^1(\Omega)/\mathbb{R}$

such that

$$-(\nabla r, \nabla z) = (g, z) \qquad \forall z \in H_0^1(\Omega), \tag{6.7}$$

$$a((u,\beta),(v,\eta)) + (\operatorname{curl} p, \eta) = (f, v) + (m, \eta) - (\nabla r, \eta) \qquad \forall\, (v,\eta) \in H_0^1(\Omega)^2 \times H_0^1(\Omega)^2, \tag{6.8}$$

$$(\beta, \operatorname{curl} q) - \frac{t^2}{\kappa}\,(\operatorname{curl} p, \operatorname{curl} q) = 0 \qquad \forall q \in H^1(\Omega)/\mathbb{R}, \tag{6.9}$$

$$(\nabla w, \nabla s) = (\beta, \nabla s) - \frac{t^2}{\kappa}\,(\nabla r, \nabla s) \qquad \forall s \in H_0^1(\Omega). \tag{6.10}$$

This is a well posed problem. In fact, first, r is the unique solution to the Dirichlet problem (6.7). Then, subtracting (6.9) from (6.8), since $t > 0$, existence and uniqueness of (u, β) and p follows from Lax-Milgram lemma. Finally, w is the solution to the well posed problem (6.10).

For $t = 0$, equations (6.7)–(6.10) also make sense, but the terms $(\operatorname{curl} p, \eta)$ from (6.8) and $(\beta, \operatorname{curl} q)$ from (6.9) must be understood weakly. Thus, in this case, we are led to finding $r_0, w_0 \in H_0^1(\Omega)$, $u_0, \beta_0 \in H_0^1(\Omega)^2$, and $p_0 \in L^2(\Omega)/\mathbb{R}$ such that

$$-(\nabla r_0, \nabla z) = (g, z) \qquad \forall z \in H_0^1(\Omega), \tag{6.11}$$

$$a((u_0,\beta_0),(v,\eta)) + (p_0, \operatorname{rot} \eta) = (f, v) + (m, \eta) - (\nabla r_0, \eta) \qquad \forall\, (v,\eta) \in H_0^1(\Omega)^2 \times H_0^1(\Omega)^2, \tag{6.12}$$

$$(\operatorname{rot} \beta_0, q) = 0 \qquad \forall q \in L^2(\Omega)/\mathbb{R}. \tag{6.13}$$

$$(\nabla w_0, \nabla s) = (\beta_0, \nabla s) \qquad \forall s \in H_0^1(\Omega). \tag{6.14}$$

This is a well posed problem, too. In fact, equations (6.11) and (6.7) are the same, so that $r_0 = r$, as well. Existence and uniqueness of (u_0, β_0) and p_0 follows from the fact that (6.12)–(6.13) is a well posed mixed problem (a is elliptic in the whole space and the *inf-sup* condition is essentially the same as that of the Stokes problem). Finally w_0 is the solution of the Dirichlet problem (6.14). Moreover the following additional regularity holds.

Lemma 6.2. *Let $(r_0, u_0, \beta_0, p_0, w_0)$ be the solution to problem (6.11)–(6.14). Then, $r_0, w_0 \in H^2(\Omega)$, $u_0, \beta_0 \in H^2(\Omega)^2$, $p_0 \in H^1(\Omega)$, and*

$$\|r_0\|_2 + \|u_0\|_2 + \|\beta_0\|_2 + \|p_0\|_1 + \|w_0\|_2 \le C\,\|(f, m, g)\|_0\,, \tag{6.15}$$

with a constant C independent of f, m, and g.

Proof. The standard *a priori* estimate for the Poisson equation on a convex domain, implies that $r_0 \in H^2(\Omega)$ and

$$\|r_0\|_2 \le C\,\|g\|_0\,. \tag{6.16}$$

Next, we write (6.12)–(6.13) in the distributional sense:

$$\begin{cases} -\bar\mu_1 \Delta u_0 - \left(\bar\lambda_1 + \bar\mu_1\right) \nabla\,(\operatorname{div} u_0) - \bar\mu_2 \Delta \beta_0 - \left(\bar\lambda_2 + \bar\mu_2\right) \nabla\,(\operatorname{div} \beta_0) = f, \\ -\bar\mu_2 \Delta u_0 - \left(\bar\lambda_2 + \bar\mu_2\right) \nabla\,(\operatorname{div} u_0) - \bar\mu_3 \Delta \beta_0 - \left(\bar\lambda_3 + \bar\mu_3\right) \nabla\,(\operatorname{div} \beta_0) \\ \qquad\qquad + \operatorname{curl} p_0 = m - \nabla r_0, \\ \operatorname{rot} \beta_0 = 0, \end{cases}$$

with Dirichlet homogeneous boundary conditions for u_0 and β_0 and the coefficients $\bar\lambda_i$ and $\bar\mu_i$, $i = 1, 2, 3$, as defined in (6.4).

The third equation above implies that $\beta_0 = \nabla\varphi$, with $\varphi \in H_0^1(\Omega)$ such that $\frac{\partial\varphi}{\partial n} = 0$ on $\partial\Omega$. Using this in the first and second equations, we obtain

$$-\bar{\mu}_1\Delta u_0 - \left(\bar{\lambda}_1 + \bar{\mu}_1\right)\nabla\left(\operatorname{div} u_0\right) - \left(\bar{\lambda}_2 + 2\bar{\mu}_2\right)\Delta\left(\nabla\varphi\right) = f, \tag{6.17}$$

$$-\bar{\mu}_2\Delta u_0 - \left(\bar{\lambda}_2 + \bar{\mu}_2\right)\nabla\left(\operatorname{div} u_0\right) - \left(\bar{\lambda}_3 + 2\bar{\mu}_3\right)\Delta\left(\nabla\varphi\right) + \operatorname{curl} p_0 = m - \nabla r_0, \tag{6.18}$$

with homogeneous boundary conditions $u_0 = 0$, $\beta_0 = 0$, $\varphi = 0$ and $\frac{\partial\varphi}{\partial n} = 0$ on $\partial\Omega$.

Taking divergence in the first two equations, we have

$$\begin{aligned} -\left(\bar{\lambda}_1 + 2\bar{\mu}_1\right)\operatorname{div}\left(\Delta u_0\right) - \left(\bar{\lambda}_2 + 2\bar{\mu}_2\right)\Delta^2\varphi &= \operatorname{div} f, \\ -\left(\bar{\lambda}_2 + 2\bar{\mu}_2\right)\operatorname{div}\left(\Delta u_0\right) - \left(\bar{\lambda}_3 + 2\bar{\mu}_3\right)\Delta^2\varphi &= \operatorname{div} m - \Delta r_0. \end{aligned}$$

Eliminating u_0 we arrive at the following problem for φ:

$$\begin{cases} K\Delta^2\varphi = \left(\bar{\lambda}_2 + 2\bar{\mu}_2\right)\operatorname{div} f - \left(\bar{\lambda}_1 + 2\bar{\mu}_1\right)\left(\operatorname{div} m - \Delta r_0\right) \in H^{-1}(\Omega), \\ \varphi = \dfrac{\partial\varphi}{\partial n} = 0 \quad \text{on } \partial\Omega. \end{cases}$$

with $K := \left(2\bar{\mu}_1 + \bar{\lambda}_1\right)\left(2\bar{\mu}_3 + \bar{\lambda}_3\right) - \left(2\bar{\mu}_2 + \bar{\lambda}_2\right)^2$, which can be shown to be strictly positive by using (6.4) and a little algebra. Therefore, from the standard *a priori* estimate for the biharmonic equation in convex domains, we know that $\varphi \in H^3(\Omega)$ and

$$\|\varphi\|_3 \le C\left(\|\operatorname{div} f\|_{-1} + \|\operatorname{div} m\|_{-1} + \|\Delta r_0\|_0\right) \le C\,\|(f,m,g)\|_0\,,$$

where we have used (6.16) for the last inequality. Therefore $\beta_0 = \nabla\varphi \in H^2(\Omega)^2$.

Next, using the last inequality in (6.17), we obtain from the usual *a priori* estimate for the elasticity problem in a polygonal convex domain that $u_0 \in H^2(\Omega)^2$ and

$$\|u_0\|_2 \le C\,\|(f,m,g)\|_0\,.$$

Now, from this inequality and (6.18), we obtain that $p_0 \in H^1(\Omega)$ and the corresponding estimate. Finally, the regularity of w_0 follows again from the standard *a priori* estimate for the Poisson equation on a convex domain applied to (6.14). Thus we conclude the proof. □

Corollary 6.3. *The solution of the limit problem (2.4) satisfies $u_0, \beta_0 \in H^2(\Omega)^2$, $w_0 \in H^2(\Omega)$, $\gamma_0 \in L^2(\Omega)^2$, and the a priori estimate (2.5) holds true.*

Proof. In this case, the Helmholtz decomposition (6.6) holds in a distributional sense (cf. [6, Proposition 3.4]):

$$\gamma_0 = \nabla r_0 + \operatorname{curl} p_0,$$

with $r_0 \in H_0^1(\Omega)$ and $p_0 \in L^2(\Omega)/\mathbb{R}$. Then, problem (2.4) is equivalent to (6.11)–(6.14), with $f = m = 0$. Hence, the additional regularity result follows from Lemma 6.2 and the above equation. □

Now we are ready to prove the *a priori* estimate for the solution to problem (6.7)–(6.10) and, consequently, to that of problem (6.5), which is the main goal of this Appendix.

Lemma 6.4. *For any $t > 0$, let (r, u, β, p, w) be the solution to problem (6.7)–(6.10). Then, $r, w, p \in H^2(\Omega)$, $u, \beta \in H^2(\Omega)^2$, and*

$$\|r\|_2 + \|u\|_2 + \|\beta\|_2 + \|p\|_1 + t\,\|p\|_2 + \|w\|_2 \le C\left(\|f\|_0 + \|m\|_0 + \|g\|_0\right),$$

with a constant C independent of t, f, m, and g.

Proof. Let $(r_0, u_0, \beta_0, p_0, w_0)$ be the solution to problem (6.11)–(6.14). Recall that $r = r_0$, so that we have already proved in Lemma 6.2 the estimate for r (cf. (6.16)).

Now, since according to Lemma 6.2, $p_0 \in H^1(\Omega)$, from (6.8)–(6.9) and (6.12)–(6.13), we obtain

$$a((u-u_0, \beta-\beta_0), (v, \eta)) + (\operatorname{curl}(p-p_0), \eta) - (\beta-\beta_0, \operatorname{curl} q) + \frac{t^2}{\kappa}(\operatorname{curl}(p-p_0), \operatorname{curl} q) = -\frac{t^2}{\kappa}(\operatorname{curl} p_0, \operatorname{curl} q)$$

for all $v, \eta \in H_0^1(\Omega)^2$ and all $q \in H^1(\Omega)/\mathbb{R}$. Testing this equation with $v := u - u_0$, $\eta := \beta - \beta_0$, and $q =: p - p_0$ and using the ellipticity of a, we have

$$\|u-u_0\|_1^2 + \|\beta-\beta_0\|_1^2 + t^2 \|p-p_0\|_1^2 \le Ct^2 \|p_0\|_1 \|p-p_0\|_1$$

and, from this estimate and (6.15), we arrive at

$$\|u-u_0\|_1 + \|\beta-\beta_0\|_1 + t\|p-p_0\|_1 \le Ct \|(f,m,g)\|_0 . \tag{6.19}$$

Hence also

$$\|p\|_1 \le \|p-p_0\|_1 + \|p_0\|_1 \le C \|(f,m,g)\|_0 . \tag{6.20}$$

Next, we apply Lemma 6.1 to (6.8) with $F := f$ and $G := m - \nabla r - \operatorname{curl} p$, to show that $u, \beta \in H^2(\Omega)^2$ and

$$\|u\|_2 + \|\beta\|_2 \le C \|(f,m,g)\|_0 ,$$

where we have used (6.16) and (6.20).

On the other hand, from (6.9) and (6.13), we have that

$$(\operatorname{curl} p, \operatorname{curl} q) = \frac{\kappa}{t^2}(\beta-\beta_0, \operatorname{curl} q) = (\operatorname{rot}(\beta-\beta_0), q) \qquad \forall q \in H^1(\Omega).$$

Therefore, p is the solution of the Neumann problem

$$\begin{cases} \Delta p = \dfrac{\kappa}{t^2} \operatorname{rot}(\beta-\beta_0) & \text{in } \Omega, \\ \dfrac{\partial p}{\partial n} = 0 & \text{on } \partial\Omega. \end{cases}$$

Hence, since Ω is convex we have

$$\|p\|_2 \le Ct^{-2} \|\beta-\beta_0\|_1 \le Ct^{-1} \|(f,m,g)\|_0 ,$$

the last inequality because of (6.19).

Finally, (6.10) is a Poisson equation, for which there holds the *a priori* estimate

$$\|w\|_2 \le C\left(\|\beta\|_1 + t^2 \|r\|_2\right) \le C \|(f,m,g)\|_0 ,$$

where we have used (6.16) once more. Thus we end the proof. □

We conclude with the main result of this Appendix.

Theorem 6.5. *Let Ω be a convex polygonal domain in the plane. For any $t > 0$ and $(f,m,g) \in H$, let $(u,\beta,w) \in V$ and $\gamma \in L^2(\Omega)$ be the solution to problem (6.5). Then, $u, \beta \in H^2(\Omega)^2$, $w \in H^2(\Omega)$, $\gamma \in H^1(\Omega)^2$, and there exists a constant C, independent of t and (f,m,g), such that*

$$\|u\|_2 + \|\beta\|_2 + \|w\|_2 + \|\gamma\|_0 + t\|\gamma\|_1 \le C\left(\|f\|_0 + \|m\|_0 + \|g\|_0\right).$$

Proof. This is an immediate consequence of Lemma 6.4 and the equivalence between problems (6.5) and (6.7)–(6.10), through (6.6). □

Corollary 6.6. *The solution of the load problem (2.2) satisfies* $u, \beta \in H^2(\Omega)^2$, $w \in H^2(\Omega)$, $\gamma \in H^1(\Omega)^2$, *and the a priori estimate (2.3) holds true.*

Proof. It is a direct application of the previous theorem to the particular right hand side of the first equation from (2.2). □

Acknowledgment

The authors thank Monique Dauge for suggesting the use of reference [12] to prove the regularity results in the Appendix and Carlos Reales for providing the axisymmetric 3D code for the numerical test from Section 4.3.

References

[1] D.N. Arnold and R.S. Falk, *A uniformly accurate finite element method for the Reissner-Mindlin plate*, SIAM J. Numer. Anal., **26** (1989) 1276–1290.

[2] F. Auricchio, C. Lovadina, and E. Sacco, *Analysis of mixed finite elements for laminated composite plates* Comput. Methods Appl. Mech. Engrg., **190** (2000) 4767–4783.

[3] F. Auricchio and E. Sacco, *A mixed-enhanced finite element for the analysis of laminated composite plates*, Internat. J. Numer. Methods Engrg., **44** (1999) 1481–1504.

[4] I. Babuška and J. Osborn, *Eigenvalue problems*, in *Handbook of Numerical Analysis*, Vol. II, P.G. Ciarlet and J.L. Lions, eds., North-Holland, Amsterdam, 1991, pp. 641–787.

[5] K.J. Bathe and E.N. Dvorkin, *A four-node plate bending element based on Mindlin/Reissner plate theory and a mixed interpolation*, Internat. J. Numer. Methods Engrg., **21** (1985) 367–383.

[6] F. Brezzi and M. Fortin, *Mixed and Hybrid Finite Element Methods*, Springer-Verlag, New York, 1991.

[7] D. Chenais and J.-C. Paumier, *On the locking phenomenon for a class of elliptic problems*, Numer. Math., **67** (1994) 427–440.

[8] R. Durán, E. Hernández, L. Hervella-Nieto, E. Liberman, and R. Rodríguez, *Error estimates for low-order isoparametric quadrilateral finite elements for plates*. SIAM J. Numer. Anal., **41** (2003) 1751–1772.

[9] R. Durán, L. Hervella-Nieto, E. Liberman, R. Rodríguez, and J. Solomin, *Approximation of the vibration modes of a plate by Reissner-Mindlin equations*, Math. Comp., **68** (1999) 1447–1463.

[10] R. Durán and E. Liberman, *On mixed finite element methods for Reissner Mindlin Plate model* Math. Comp., **58** (1992) 561–573.

[11] T. Kato, *Perturbation Theory for Linear Operators*, Springer Verlag, Berlin, 1995.

[12] V. Kozlov, V. Maz'ya, and J. Rossmann, *Spectral Problems Associated with Corner Singularities of Solutions to Elliptic Equations*, Mathematical Surveys and Monographs **85**, AMS, Providence, RI, 2001.

[13] O.O. Ochoa and J.N. Reddy, *Finite element analysis of composite laminates*, Kluwer Academic Publishers, Dordrecht, The Netherlands, 1992.

[14] P.A. Raviart and J.M. Thomas, *A mixed finite element method for 2nd order elliptic problems*, in *Mathematical Aspects of Finite Element Methods* Lecture Notes in Mathematics **606**, Springer, Berlin, 1977, pp. 292–315.

[15] J.N Reddy, *Energy and Variational Methods in Applied Mechanics*, Wiley, New York, 1984.

[16] J.N Reddy, *Mechanics of Laminated Composite Plates – Theory and Analysis*, CRC Press, Boca Raton, 1997.

Departamento de Matemática, Facultad de Ciencias Exactas y Naturales, Universidad de Buenos Aires, 1428 - Buenos Aires, Argentina.
E-mail address: rduran@dm.uba.ar

CI^{2}MA, Departamento de Ingeniería Matemática, Universidad de Concepción, Casilla 160-C, Concepción, Chile.
E-mail address: rodolfo@ing-mat.udec.cl

Departamento de Ingeniería Matemática, Universidad de Concepción, Casilla 160-C, Concepción, Chile.
E-mail address: fsanhuez@ing-mat.udec.cl